TRITA-EPP-79-21

ELECTROSTATIC DOUBLE LAYERS AND A PLASMA EVACUATION PROCESS

M.A. Raadu and P. Carlqvist

December 1979

Department of Plasma Physics
Royal Institute of Technology
S-100 44 Stockholm, Sweden

ELECTROSTATIC DOUBLE LAYERS AND A PLASMA EVACUATION PROCESS

Michael A. Raadu and Per Carlqvist

Department of Plasma Physics, Royal Institute of Technology,
S-100 44 Stockholm, Sweden

Abstract

An evacuation process due to the growth of current driven instabilities in a plasma is discussed. The process, which leads to localized extreme density reductions, is related to the formation of electrostatic double layers. The initial linear phase is treated using the superposition of unstable plasma waves. In the long wave length, non-dispersive limit a density dip, which is initially present as a small disturbance, grows rapidly and remains localized in the plasma. The process works for a variety of plasma conditions provided a certain current density is exceeded. For a particular choice of plasma parameters the non-linear development is followed, by solving the coupled Vlasov-Poisson equations by finite difference methods. The evacuation process is found to work even more effectively in the non-linear phase and leads to an extreme density reduction within the dip. It is suggested that the growth of such structures produces weak points within the plasma that can lead to the formation of double layers.

1. Introduction

Plasmas which carry large electric currents are known to be subject to a variety of instabilities,the growth of which may lead to drastic changes in their properties. One possibility is that the instabilities give rise to large amplitude waves that interact with one another and establish a steady state. It has been suggested that such waves scatter particles and impede the current so that the plasma develops an anomalously high resistivity (Buneman, 1958, 1959). A number of experiments have been performed to study anomalous resistivity (for a review see Schrijver, 1973). For the theoretical study of this phenomenon it has usually been assumed that the plasma has a scale length much greater than the wave-lengths considered. The enhanced electric field necessary to maintain the current in the disturbed plasma can then be expected to exist over an extended region.

Another possibility for the development of current driven instabilities is that they will lead to the formation of electrostatic double layers. The double layer represents a local region in the plasma capable of sustaining high potential drops ($\phi_{DL} \gtrsim \kappa T/e$, where T is the plasma temperature). Basically it consists of two adjacent layers - one with an excess of positive charges and the other with an excess of negative charges. Strong electric fields exist inside the double layer. Outside the layer, however, the electric field is much weaker implying that the layer taken as a whole is practically neutral. The thickness of the double layer is generally much smaller than the mean free paths of the charged particles. Hence, collisional effects are of minor importance within the layer. The double layer can therefore be described using the Vlasov and Poisson equations combined.

A schematic picture of the ion and electron distributions in a double layer is shown in Figure 1. Both free and reflected particles are needed to build up the layer. The current through the layer is carried by the free particles. Some of the free ions and electrons are accelerated and form beams on opposite sides of the laver. A basic requirement is that the potential drop across the double layer (Figure 1a) must be maintained by external sources. For recent reviews on double layers see Block (1978), Carlqvist (1979), and Torvén (1979).

In several experiments it has been demonstrated that double layers are formed when the current density in the initial plasma exceeds a certain critical value (Babić and Torvén, 1974; Quon and Wong, 1976; Torvén, 1979). In some cases it is observed that large amplitude waves develop in the plasma immediately before the formation phase (Torvén and Babić, 1975; Quon and Wong, 1976). The formation of double layers has been studied by computer simulation of a plasma (Joyce and Hubbard, 1978). The electron density within a double layer has been found experimentally to be considerably less than in the surrounding plasma (Lindberg and Torvén, 1979). This density reduction can be understood from theoretical models of double layer structure (e.g. see Nyberg, 1979). Since double layers are essentially regions of reduced density across which particles are accelerated there are therefore good reasons to assume that some current dependent instability, leading to a local evacuation of the plasma, is of decisive importance for the formation of double layers (Alfvén and Carlqvist, 1967). DeGroot et al. (1977) find in a computer study that regions of low density favour the formation of double layers.

Several different evacuation instabilities may serve as initiators of double layers. In the present article we shall study more closely an evacuation produced by the two-stream or ion-acoustic instabilities. We can easily describe the linear phase of the evacuation process if we consider a fully ionized, cold ($T_e = T_i = 0$) and one-dimensional plasma in which the electrons move relative to the ions with a velocity u (Carlqvist, 1973). The plasma is assumed to be homogeneous everywhere except for a small localised density disturbance in the form of a dip. The density dip can be thought of as being built up of a continous set of waves forming a Fourier representation of the dip. Some of the waves grow as a result of the two-stream instability. In the linear phase these unstable waves grow in amplitude independently of each other. Hence, the Fourier spectrum changes progressively. From the time development of the spectrum it is then possible to deduce how the density disturbance evolves.

A particularly simple case to study is that of a density dip which has a scale-length that is long compared to u/ω_{pe} (where ω_{pe} is the electron plasma frequency). In this case, where the phase velocity of the Fourier waves is approximately constant, the development of the spectrum leads to a simultaneous deepening and narrowing of the dip.

In the following we shall see that this evacuation process is active not only in cold plasmas but also when the ions and electrons in the plasma have finite temperatures. Furthermore, by means of numerical methods we shall study how the evacuation proceeds in the non-linear phase.

2. Linear Development

As discussed above, an evacuation process can be shown to result from the linear growth of nearly non-dispersive plasma waves. This process occurs equally well both in hot and cold plasmas. Before treating the non-linear case we shall first consider the marginal instability condition, growth rate γ, and phase velocity v_ϕ in the linear case. The results obtained will be applied to demonstrate the growth of a local density dip.

We consider a fully ionized plasma consisting of counterstreaming ions and electrons with Maxwellian velocity distributions. In the frame of the ions small amplitude electrostatic waves of the form $\exp i(kx - \omega t)$ (wavenumber k, frequency $\omega = \omega_r + i\gamma$) then satisfy the dispersion relation

$$k^2 + \frac{\omega_{pi}^2}{c_i^2} I\left(\frac{\omega}{\sqrt{2}\, kc_i}\right) + \frac{\omega_{pe}^2}{c_e^2} I\left(\frac{\omega - ku}{\sqrt{2}\, kc_e}\right) = 0 \qquad (2.1)$$

given by Stringer (1964), where ω_{pi} is the plasma frequency $c_i = \kappa T_i/m_i$ the ion r.m.s. random velocity and similarly for the electrons (see also Jackson, 1960). The function I is known and has been tabulated (see e.g. Fried and Conte, 1961). When the relative drift velocity u between ions and electrons exceeds a certain value, which depends on the temperatures T_e and T_i, the waves are known to be unstable.

A variety of different methods depending on the electron and ion temperatures have been used to find the properties of unstable waves subject to the basic dispersion relation (2.1). For the cold case ($T_e = T_i = 0$) this relation reduces to a simple algebraic form derived by Buneman (1958, 1959) from which the wave properties may be derived directly. In the limit of extreme temperature ratios ($T_e/T_i \gg 1$ or $T_e/T_i \ll 1$) analytic approximations have been found (Jackson, 1960). Numerical methods are necessary in the case of a finite temperature ratio and in particular for the equal temperature case ($T_e = T_i$) where the zero of the real part of the function I must be found to determine the condition for marginal instability (Buneman, 1959). In general, analytic approximations may be found in the neighbourhood of any particular solution of equation (2.1) using power series expansions of the function I (cf. Clemmow and Dougherty, 1969). Here we are interested in the properties of long wavelength instabilities ($k \to 0$). Some of these properties are displayed in Table I for particular choices of the electron and ion temperatures. This table is constructed using results given in the above references and analytic approximations that may be derived from them.

In all the cases shown the waves are nearly non-dispersive ($v_\phi \approx$ constant) in the limit of long wavelengths ($k \to 0$). In general the relative drift velocity u_m for marginal instability depends on the wavenumber considered. Thus there are unstable waves if

$$u > u_m(k) \quad . \qquad (2.2)$$

For equal temperatures the minimum value of u_m occurs for $k = 0$ but for extreme temperature ratios ($T_e/T_i >> 1$ or $T_e/T_i << 1$) the minimum occurs for $|k| > 0$ (see Jackson, 1960). In all the cases displayed in Table I the growth rate γ in the limit of long wavelengths is given by

$$\gamma = A|k| \tag{2.3}$$

where the factor A is a constant determined by the properties of the plasma. Thus the growth rate is approximately proportional to the wavenumber.

The density dip $\Delta n(x,t)$, being a function of space and time, may now be treated as a superposition of nearly non-dispersive waves with growth rates given by equation (2.3) for a variety of plasma conditions. The length scale should be sufficiently great so that the long wavelength approximation can be used. To show the typical development of a density dip we shall consider a specific case where the initial ($t = 0$) density perturbation has a Gaussian profile (Figure 2a, the solid curve)

$$\Delta n(x,o) = -\Delta n_o \exp\left(-\frac{1}{2}\frac{x^2}{L^2}\right) \tag{2.4}$$

where L is a measure of the width of the dip. The symmetric Fourier transform of this dip is then

$$\widehat{\Delta n}(k,o) = \frac{1}{\sqrt{2\pi}}\int_{-\infty}^{+\infty} \Delta n(x,o)\, e^{-ikx} dx = \Delta n_o L \exp\left(-\frac{1}{2} L^2 k^2\right) \tag{2.5}$$

(see Figure 2b, the solid curve). Since the length scale L is assumed to be long the associated waves grow according to equation (2.3) and the Fourier transform at a time t becomes

$$\widehat{\Delta n}(k,t) = -\Delta n_o L \exp\left(-\frac{1}{2} L^2 k^2 + A|k|t\right) \tag{2.6}$$

(see Figure 2b, the dashed curve). The corresponding density dip is then found by Fourier inversion to be

$$\Delta n(x,t) = -\Delta n_o \, \mathrm{Re}\{e^{-z^2} \operatorname{erfc}(-iz)\} \tag{2.7}$$

where $z = (x - v_\phi t - iAt)/(L\sqrt{2})$. The function erfc is the error function (see for example Abramowitz and Stegun, 1965). As may be seen from Figure 2a (the dashed curve) the dip deepens and becomes narrower. It can be shown that for $t > 1.65\ t_1$, where $t_1 = \sqrt{2}\ L/A$, the central value of the density dip Δn_c is approximately $2\Delta n_o \exp\left[(t/t_1)^2\right]$ to within 1%. The time t_1 is thus a characteristic time for the development of the dip. It may be seen that this development is faster than exponential.

These linear results thus show that the growth of non-dispersive waves leads to an increase in amplitude of local rarefactions. Since the growth rate is greater for large wave numbers (Equation 2.3) the region of low density becomes narrower as the density falls. Therefore there seems to be a natural tendency for local regions of low density to develop in unstable current carrying plasmas.

3. The Non-linear Development

3.1 Choice of the non-linear case

To establish the physical significance of the evacuation mechanism it is necessary to extend the treatment from the linear into the non-linear phase. In particular it is important to find out whether or not there are non-linear saturation mechanisms which could stop the process or dispersive effects that might destroy the structure.

In the following we shall study numerically the non-linear phase of the evacuation process using the Vlasov and Poisson equations. One of the most convenient cases for such a study has proved to be the cold electron case ($T_e = 0$, $T_i \neq 0$) with the scale length ℓ of the density disturbance being large compared to the Debye length in the plasma λ_D. For a realistic electron to ion mass ratio $\mu = m_e/m_i \ll 1$, the time for electrons to cross the dip is much shorter than the growth time of the instability and their motion is approximately steady. On the other hand the zero temperature of the electrons implies that no electrons will be trapped. The electrons may therefore be treated as a cold fluid having a steady motion. Furthermore for the large scale-lengths considered the electron density closely follows the ion density. These properties are all favourable for a non-linear numerical analysis. Thus a realistic value of the electron to ion mass ratio can be adopted, while at the same time the integration time and length steps can be kept large compared to the electron plasma period (ω_{pe}^{-1}) and the Debye length respectively. For these practical reasons we choose the cold electron case with long scale-lengths for non-linear treatment.

3.2 The basic equations

For the non-linear treatment we consider a one-dimensional and collisionless cold-electron plasma ($T_e = 0$, $T_i \neq 0$). The electrons are assumed to have a steady motion with a velocity v_e and density n_e satisfying the continuity equation

$$\frac{\partial (n_e v_e)}{\partial x} = 0 \qquad (3.1)$$

and the momentum equation

$$m_e v_e \frac{\partial v_e}{\partial x} = - eE \qquad (3.2)$$

where E is the electric field. If the electron current density is $i_e = - en_e v_e$ the electric field can be found from equations (3.1) and (3.2) yielding

$$E = - \frac{\partial}{\partial x} \left(\frac{m_e i_e^2}{2n_e^2 e^3} \right) \quad . \qquad (3.3)$$

For sufficiently great length scales $\ell >> \lambda_D$ there is approximate charge neutrality, $n_e \simeq n_i$. Equation (3.3) then implies a direct relationship between the electric field and the ion density.

The ions are assumed to have a spread in velocities described by the ion phase space density $f_i(x,v,t)$. The ion motion then satisfies the Vlasov equation

$$\frac{\partial f_i}{\partial t} + v \frac{\partial f_i}{\partial x} + \frac{eE}{m_i} \frac{\partial f_i}{\partial v} = 0 \qquad (3.4)$$

and the ion density is given by

$$n_i(x,t) = \int_{-\infty}^{+\infty} f_i(x,v,t)\, dv \quad . \qquad (3.5)$$

To find solutions of the above equations we must specify the initial ion phase space density $f_i(x,v,o)$ and appropriate boundary conditions for the Vlasov equation (3.4).

3.3 The physical interpretation

By means of the equations (3.1) to (3.5) we can clarify the way in which the density dip develops in the non-linear phase. We begin by looking at the ions and assume that they have a given initial phase space density consistent with a local density dip in an otherwise homogeneous plasma (cf. equation (3.5)). As a result of approximate charge neutrality (see Section 3.2) there will also be a similar dip in the electron density. Since there is a constant electron current density (see equation (3.1)) there must be a corresponding acceleration and deceleration of electrons crossing the dip. This requires an electric field as given by equation (3.3). However, this electric field also acts upon the ions giving rise to a progressive change of their phase space density f_i (see equation (3.4)).

3.4 The numerical method

The system of equations (3.1) to (3.5) can be solved numerically using finite difference methods. A two dimensional grid is used to represent a limited region of phase space, $|x| \leq x_o$, $|v| < v_o$. The grid points are equally spaced in position x and in velocity v, the separation being Δx and

Δv respectively. The ion phase space density $f_i(x,v,t)$ is represented by its values at the grid points.

In order to perform the time integration of the Vlasov equation (3.4) we use a generalisation of the Lax-Wendroff one-dimensional scheme (Lax and Wendroff, 1960). Such a scheme ensures that the total number of ions is well conserved during their motion, although fine details of their phase space density are less well resolved.

In a time interval Δt the ion phase space density will change by an amount Δf_i in accordance with equation (3.4). We first find the contribution to Δf_i from the second term, using the one-dimensional Lax-Wendroff scheme

$$\Delta f_x(x,v,t) = -\frac{v\Delta t}{2\Delta x}\left[f_i(x+\Delta x,v,t) - f_i(x-\Delta x,v,t)\right]$$

$$+\frac{v^2\Delta t^2}{2\Delta x^2}\left[f_i(x+\Delta x,v,t) - 2\,f_i(x,v,t) + f_i(x-\Delta x,v,t)\right] \quad . \qquad (3.6)$$

The contribution Δf_v from the third term in equation (3.4) is found in a similar way, but using $(f_i + \Delta f_x)$ instead of f_i alone. This method ensures numerical stability (cf. Killeen and Rompel, 1966). At each grid point the total change is

$$\Delta f_i = \Delta f_x + \Delta f_v \quad . \qquad (3.7)$$

In order to obtain meaningful results the size of the time step Δt used in calculating Δf_x and Δf_v has to be limited by the CFL-condition (Courant, Friedrichs, and Lewy, 1928). This condition means that a particle at any grid point (x,v) must not move outside the cell $(x \pm \Delta x,\ v \pm \Delta v)$ within the time step Δt. Hence, we require

$$\Delta t < \frac{\Delta z}{|v|} \qquad (3.8)$$

and

$$\Delta t < \frac{m_i \Delta v}{e|E|} \qquad (3.9)$$

at all grid points (x,v). These conditions are checked at each time step in the computation and the value of Δt is reduced if necessary.

The initial conditions are fully specified once the ion phase space density at zero time, $f_i(x,v,o)$, is chosen. At the spatial boundaries of the grid $x = \pm x_o$ ions both enter and leave the system. However, one is only free to specify the distribution over velocity of the incoming particles. Here we will assume for physical reasons explained later (see Section 3.5), that these distributions are constant in time so that

$$f_i(-x_o,v,t) = f_i(-x_o,v,o) \qquad \text{for } v > 0 \qquad (3.10)$$

and

$$f_i(x_o,v,t) = f_i(x_o,v,o) \qquad \text{for } v < 0 \ . \qquad (3.11)$$

One is also free to specify the value of the phase space density for particles entering across the velocity boundaries $v = \pm v_o$ of the grid. Here we assume this value to be zero at all times so that

$$f_i(x,v_o,t) = 0 \qquad \text{for } \frac{eE}{m_i} < 0 \qquad (3.12)$$

and

$$f_i(x,-v_o,t) = 0 \qquad \text{for } \frac{eE}{m_i} > 0 \ . \qquad (3.13)$$

The integral over velocity giving the ion density (equation (3.5)) is evaluated by Simpson's rule at each time step. The electric field E then follows from the finite difference form of equation (3.3). The acceleration due to this field allows Δf_v in equation (3.7) to be calculated and hence the change in the ion distribution function Δf_i is found in a self-consistent way.

3.5 Physical conditions and numerical results

We study numerically the non-linear development of a local density dip within a homogeneous plasma of density n_o. Initially the dip has a Gaussian profile with an amplitude $\Delta n_o = 0.2\ n_o$ and a length scale L. This corresponds to the problem treated linearly in Section 2. The ions are initially assumed to have a Maxwellian velocity distribution with a uniform temperature T_i and to have no systematic velocity. We envisage the development of the local density dip as taking place in an extended region of homogeneous plasma. For practical reasons the numerical treatment has to be restricted to a limited region. The spatial boundaries are chosen so that the plasma there remains undisturbed during the time interval considered. This is consistent with the external homogeneous plasma remaining undisturbed and with the boundary condition (3.10) and (3.11) for ions entering the region. The velocity boundaries are chosen to be at $v = \pm\ v_o = \pm\ 4c_i$ so that the value of the distribution function there $f_i(v_o)$ is sufficiently small so as not to influence the results.

In order to demonstrate the evacuation process the velocity of the cold electrons must exceed the marginal value for instability. From Table I the marginal value for linear growth is $u_m = c_i/\sqrt{\mu}$. Thus we choose the electron velocity outside the density dip to be $v_{eo} = 1.4\ u_m$.

The development of the density profile and the phase space density found from the numerical calculations are illustrated in Figures 3 to 8. The sequence is shown for a selection of times ranging from $t = 0$ to $t = 1.08\ L/c_i$. The times are given in terms of a natural unit L/c_i corresponding to the time needed for an ion having the mean thermal velocity to travel the typical length scale L of the original disturbance. The density at the centre of the dip decreases progressively and at a time $t = 1.08\ L/c_i$ it is less than one third of the homogeneous density n_o.

The evacuation process is seen to be accompanied by a considerable narrowing of the density dip. Hence, we may conclude that the plasma removed from the central parts of the dip is first of all deposited in the immediate vicinity thus filling in the wings of the density profile. As is evident from the Figures there is little or no increase of the density above the homogeneous value n_o.

It should be noticed that during the time interval considered there is no appreciable density disturbance near the boundaries $x = \pm 4$ L despite the considerable reduction of density within the dip. Thus the evacuation process remains strongly localised even in the non-linear phase.

The phase space density of the ions corresponding to the density profiles discussed above is also given in Figures 3 to 8 for the same selected times. The contour levels are plotted for a set of phase space density values (0.2 - 0.8) using an interpolation on the values found at the grid points (Mehra, 1973). For the interpretation of these figures it should be noted that the contour level 0.6 closely corresponds to those ions with the mean thermal velocity c_i in the undisturbed plasma. As may be seen from figures 4 to 8 the contours of the phase space density on the right-hand side are progressively displaced upwards in the neighbourhood of the dip. On the left-hand side the displacement is downwards. This means that ions are accelerated away from the centre of the disturbance leading to the local evacuation evident from the density profiles. At the later stages of the evacuation process (Figures 7 to 8) the displacement of the contours close to the centre is so great that most of the ions are there moving outwards. However, on the spatial boundaries, $x = \pm 4$ L, there is no detectable displacement which means that the particles arriving there from the plasma region considered have not experienced any appreciable acceleration. This shows that the plasma on the spatial boundaries remains essentially undisturbed as required for the boundary conditions (3.10) and (3.11). Hence, there is practically no net flux of particles across the spatial boundaries. Moreover, since the velocity boundaries $v = \pm v_o$ are chosen so that there is a negligible outflux of particles there, the total number of particles within the region should be nearly constant. This is confirmed by a direct integration over phase space which shows that the total number of particles is constant within 0.03% for the time interval studied.

The decrease in the central density of the dip n_c as a function of time is shown in Figure 9. Since the ions are initially at rest the development is at first rather slow. However, towards the end of the period covered by the computations the density decreases very rapidly on a time scale which is much shorter than L/c_i. Beyond the time $t = 1.08\ L/c_i$ the characteristic length scale of the dip became too small for accurate representation with the chosen grid spacing. The calculations were therefore terminated at this point.

As may be seen from the Figures 3 to 8 the time is expressed in units of L/c_i. This means that the figures may be interpreted as showing the development of the density dip for a variety of values of L and c_i, provided that the ratio between the electron velocity outside the dip v_{eo} and the marginal velocity for growth $c_i/\sqrt{\mu}$ is kept constant.

4. Discussion

In Section 2 we treated the linear development of a localised density dip using the superposition of growing plasma waves. For sufficiently high currents the density dip becomes rapidly deeper and narrower as the result of instabilities. In the non-linear regime such a superposition of waves is not possible, but the numerical analysis described in Section 3 demonstrates that for the case of cold electrons the evacuation process works equally well. The reason for this is that in both the linear and non-linear regimes there is a common underlying physical mechanism.

The driving force of this mechanism is provided by the electron motion. Within the dip the electrons must be accelerated so that their density n_e follows the local density of the ions n_i. For cold electrons this acceleration can only be provided by an outwardly directed electric field E (see Equation (3.3)). This electric field also acts on the ions producing an outward driving force

$$F_E = en_iE = -\frac{\partial}{\partial x}(m_e n_e v_e^2) \quad . \tag{4.1}$$

In order for evacuation to occur this driving force must overcome the force due to the ion pressure gradient. Hence, it is clear that the electron velocity (current) must exceed a critical value for the instability to take place.

It is of interest to compare the shape of the density dip for the non-linear development treated in Section 3 with that for the small amplitude linear development found in Section 2. Such a comparison is made in Figure 10. Figure 10a shows the density profile for the linear development at t = 0 (the solid curve) and at $t = 1.08\ L/c_i$ (the dashed curve), using the same homogeneous plasma conditions as for the non-linear treatment. In Figure 10b the corresponding results for the non-linear treatment are reproduced (cf. Figures 3 and 8). We have chosen the density scales in Figure 10a and Figure 10b in such a way that the initial density profiles appear to be identical. This of course means that the density scales are of necessity completely different. Comparing Figures 10a and 10b it is clear that the relative increase in the amplitude of the density dip is considerably greater for the non-linear development. Another difference to be noticed is that the non-linear development results in a more narrow profile. The reason that the relative development of the density dip is faster in the non-linear regime is that the electric field E given by Equation (3.3) increases relatively more rapidly with decreasing density than in the linear regime.

The particular case of cold electrons ($T_e = 0$, $T_i \neq 0$) has here been chosen for the study of the non-linear phase of the evacuation process. This choice, as explained in Section 3.1, was made to simplify the computations while still retaining the essential physical properties. However, it is clear from Section 2 that in the linear regime the evacuation process works equally well for other ratios of the ion and electron temperatures. Therefore in these cases, we may also expect the evacuation to proceed in the non-linear regime just as in the cold electron case studied.

In the non-linear treatment presented in Section 3 we have for simplicity considered a situation in which high frequency oscillations are not present. In real plasmas, however, such oscillations are likely to be present. These oscillations may for example be generated within the dip as the result of current driven instabilities. Another possibility is that the oscillations are generated by external sources and trapped inside the dip. In both cases the electric field amplitude of the oscillations E_o may reach a maximum in the central parts of the dip. Under such conditions the oscilla-tions will give rise to a ponderomotive force

$$F_P \propto -\frac{\epsilon_o}{2} \frac{\partial E_o^2}{\partial x} \qquad (4.2)$$

which primarily acts on the electrons and is directed outwards from the centre of the dip. Although the ions are not appre-ciably affected by the oscillations, they are acted upon by an ambipolar electric field so that the whole plasma in the dip experiences the outward force F_P. Hence, an accumulation of oscillations within the dip would assist the evacuation process discussed in previous sections. The ponderomotive force F_P acting alone is regarded as the basic driving force in cavitons (Zakharov, 1972; Morales and Lee, 1974). The efficiency of the caviton process compared with the evacuation process discussed in earlier sections depends on the relative magnitude of the driving forces F_E and F_P (cf. Expressions (4.1) and (4.2)).

In this paper we have demonstrated that current driven instabilities will lead to a local drastic reduction of the plasma density, wherever there is an initial disturbance in the form of a density dip. In real plasmas many density disturbances with a variety of widths and amplitudes can be expected to be present. Some of these will develop more rapidly leading to extreme conditions in local regions. These regions may be compared to the weak links in a chain.

In the present study of the evacuation process we have assumed approximate charge neutrality ($n_e \approx n_i$) within the plasma. This condition is certainly fulfilled during the first stage of the evacuation considered here. However, when the density of the plasma has decreased to a sufficiently low value charge neutrality will be broken. The critical density at which this occurs depends both on the width of the dip and on the maximum energy of the accelerated electrons.

The further development of the density dip with a substantial charge separation has not so far been treated in any detail. One possibility that has been suggested is that it may lead to the formation of an electrostatic double layer (Alfvén and Carlqvist, 1967; Carlqvist, 1972). The dip in the plasma may be interpreted as a "double double layer" consisting of a pair of opposed double layers such that the total potential drop across both of the layers is much smaller than the potential drop across each of the layers. Each half of the dip forms a double layer with a potential drop consistently produced by the moving charges. The ions are accelerated outwards in both layers, whereas the electrons are accelerated in one layer and decelerated in the other layer. An important problem that remains to be solved is if and under what conditions such a double double layer can finally turn over into a single double layer. A thorough treatment of this problem is, however, beyond the scope of this paper.

Acknowledgements

The authors would like to thank Drs F. Čech, L. Lindberg and S. Torvén for their interest in this work and for their useful comments. This work has been supported by the Swedish Board for Space Activities, ESRO, and the Swedish Natural Science Research Council.

References

Abramowitz, M. and Stegun, I.A., Handbook of Mathematical Functions, Dover Publications, New York, p. 297, 1965.

Alfvén, H. and Carlqvist, P., Currents in the Solar Atmosphere and a Theory of Solar Flares, Solar Phys., 1, 220, 1967.

Babić, M. and Torvén, S., Current Limiting Space Charge Sheats in a Low Pressure Arc Plasma, TRITA-EPP-74-02, Dept of Plasma Phys., Royal Inst. of Tech., Stockholm, Sweden, 1974.

Block, L.P., A Double Layer Review, Astrophys. Space Sci., 55, 59, 1978.

Buneman, O., Instability Turbulence and Conductivity in Current-Carrying Plasma, Phys. Rev. Lett., 1, 8, 1958.

Buneman, O., Dissipation of Currents in Ionized Media, Phys. Rev. 115, 503, 1959.

Carlqvist, P., On the Formation of Double Layers in Plasmas, Cosmic Electrodyn., 3, 377, 1972.

Carlqvist, P., Double Layers and Two-Stream Instability in Solar Flares, TRITA-EPP-73-05, Dept of Plasma Phys., Royal Inst. of Tech., Stockholm, Sweden, 1973.

Carlqvist, P., Some Theoretical Aspects of Electrostatic Double Layers, Wave Instabilities in Space Plasmas, Astrophysics and Space Science Book Series, Ed. P.J. Palmadesso and K. Papadopoulos, D. Reidel Publ. Comp., Dordrecht - Holland, p. 83, 1979.

Clemmow, P.C. and Dougherty, J.P., Electrodynamics of Particles and Plasmas, Addison-Wesley Publ. Comp., Reading, Mass., 1969.

Courant, R., Friedrichs, K.O., and Lewy, H., Über die Partiellen Differenzengleichungen der Mathematischen Physik, Math. Ann., 100, 32, 1928.

DeGroot, J.S., Barnes, C., Walstead, A.E., and Buneman, O., Localized Structures and Anomalous dc Resistivity, Phys. Rev. Letters, 38, 1283, 1977.

Fried, B.D. and Conte, S.D., The Plasma Disperson Function, Academic Press, New York, 1961.

Jackson, E.A., Drift Instabilities in a Maxwellian Plasma, Physics of Fluids, 3, 786, 1960.

Joyce, G. and Hubbard, R.F., Numerical Simulation of Plasma Double Layers, Rep. 78-10, Dept of Phys. and Astron., U. of Iowa, Iowa City, 1978.

Killeen, J. and Rompel, S.L., A Computation for Studying the Formation of the Relativistic Electron Layer in Astron, J. Comput. Phys., 1, 29, 1966.

Lax, P.D. and Wendroff, B., Systems of Conservation Laws, Comm. Pure Appl. Math., 13, 217, 1960.

Lindberg, L. and Torvén, S., Some Characteristics of an Electric Double Layer in a Magnetized Plasma, Journal de Physique, Colloque C7, supplément au n° 7, 40, 151, 1979.

Mehra, R., Contour Plot Package User's Manual, Stockholms Datamaskincentral, Royal Inst. of Tech., Stockholm, Sweden, 1973.

Morales, G. and Lee, Y.C., Ponderomotive-Force Effects in a Nonuniform Plasma, Phys. Rev. Lett., 33, 1016, 1974.

Nyberg,C., The Electron Density Variation inside an Electrostatic Double Layer, TRITA-MEK-79-06, Dept of Mechanics, Royal Inst. of Tech., Stockholm, Sweden, 1979.

Quon, B.H. and Wong, A.Y., Formation of Potential Double Layers in Plasmas, Phys. Rev. Lett., 37, 1393, 1976.

Schrijver, H., Turbulent Resistivity in Hydrogen and Noble-Gas Plasmas, Physica, 70, 358, 1973.

Stringer, T.E., Electrostatic Instabilities in Current-Carrying and Counterstreaming Plasmas, Plasma Phys., 6, 267, 1964.

Torvén, S. and Babić, M., Current Chopping Space Charge Layers in a Low Pressure Arc Plasma, Proc. 12th Int. Conf. on Phenomena in Ionized Gases, Ed. J.G.A. Hölscher and D.C. Schram, American Elsevier Publ. Comp., New York, p. 124, 1975.

Torvén, S., Formation of Double Layers in Laboratory Plasmas, Wave Instabilities in Space Plasmas, Astrophysics and Space Science Book Series, Ed. P.J. Palmadesso and K. Papadopoulos, D. Reidel Publ. Comp., Dordrecht - Holland, p. 109, 1979.

Zakharov, V.E., Collapse of Langmuir Waves, Zh. Exsp. Teor. Fiz., 62, 1745, 1972 (Sov. Phys. - JETP, 35, 908, 1972).

Table I

The marginal velocity for instability u_m and the growth rate γ given for four different choices of the ion and electron temperature T_i and T_e in the long wavelength approximation. In all cases but for $T_e = T_i = 0$ the growth rate is calculated for a relative drift velocity u satisfying $|u - u_m| << u_m$. It is to be noticed that the growth rate is proportional to the wavenumber k in all cases.

	u_m	γ
$T_e = T_i = 0$	0	$\frac{\sqrt{m_e m_i}}{m_e + m_i} k u$
$T_e \neq 0,\ T_i = 0$	$\sqrt{\frac{\kappa T_e}{m_i}}$	$\sqrt{\frac{\pi}{8}} \sqrt{\frac{m_e}{m_i}} k(u-u_m)$
$T_e = T_i \neq 0$	$1.31(1+\sqrt{\frac{m_e}{m_i}}) \sqrt{\frac{\kappa T_e}{m_e}}$	$0.798 \sqrt{\frac{m_e}{m_i}} k(u-u_m)$
$T_e = 0,\ T_i \neq 0$	$\sqrt{\frac{\kappa T_i}{m_e}}$	$\sqrt{\frac{8}{\pi}} \sqrt{\frac{m_e}{m_i}} k(u-u_m)$

Figure captions

Fig. 1 Schematic picture of a) the potential distribution, b) phase space for the ions, and c) phase space for the electrons in a double layer surrounded by plasma. Both the ion and electron populations consist of free particles which can pass the double layer and of reflected particles which cannot penetrate the layer because of the potential barrier. The free particles are either accelerated or decelerated depending on their direction of motion relative to the electric field.

Fig. 2 Local evacuation of a current carrying plasma in the linear phase. The relative drift between the ions and electrons is supposed to be so large that a current driven electrostatic instability with the growth rate $\gamma = A|k|$ is initiated. a) shows the plasma density n as a function of the normalized space coordinate x/L while b) shows the normalized Fourier transform $\widehat{\Delta n}/L\Delta n_o$ as a function of kL. The solid curves refer to the initial state t = 0 for which the density disturbance is assumed to be $\Delta n = -\Delta n_o \exp(-x^2/2L^2)$ while the dashed curves refer to a later time $t = \sqrt{2}L/A$. As time passes the density dip becomes progressively deeper and narrower.

Fig. 3-8 Non-linear development of a density dip in a cold electron plasma ($T_e = 0$, $T_i \neq 0$) carrying the current density $i = 1.4\ en_oc_i/\sqrt{\mu}$. Each of the figures in the sequence shows a) the normalized plasma density n/n_o as a function of x/L and b) the phase space density f_i for the ions with contour levels $f_i = 0.2 - 0.8$. The figures refer to the times t = 0, $t = 0.53\ L/c_i$, $t = 0.70\ L/c_i$, $t = 0.88\ L/c_i$, $t = 1.03\ L/c_i$, and $t = 1.08\ L/c_i$. At time t = 0 the density is assumed to be $n = n_o - 0.2n_o \exp(-x^2/2L)$ with the ions having a Maxwellian velocity distribution. As is clear from the figures the ions are gradually pushed away from the centre of the dip so that the density dip becomes progressively deeper and narrower. In the last figure of the sequence the density is reduced to about one third of the density n_o far away from the dip.

Fig. 9 The central density of the dip n_c normalized to n_o shown as a function of time t normalized to L/c_i. At time t = 0 there is no change of the central density with time since the ion population has initially no mean velocity. However, as time passes the central density falls with increasing rapidity. During the last third of the time interval covered by the numerical calculations an almost catastrophic decrease of the central density is found to occur.

Fig. 10 Comparison of a) the linear phase of the evacuation and b) the non-linear phase. The density scales in a) and b), which are quite different, are chosen so that the initial (t = 0) density profiles of the linear and non-linear cases (the solid curves) exactly match each other. The dashed curves show the density profiles at time t = 1.08 L/c_i. It is to be noticed that the non-linear development leads to a deeper and more narrow density profile as compared to the linear development.

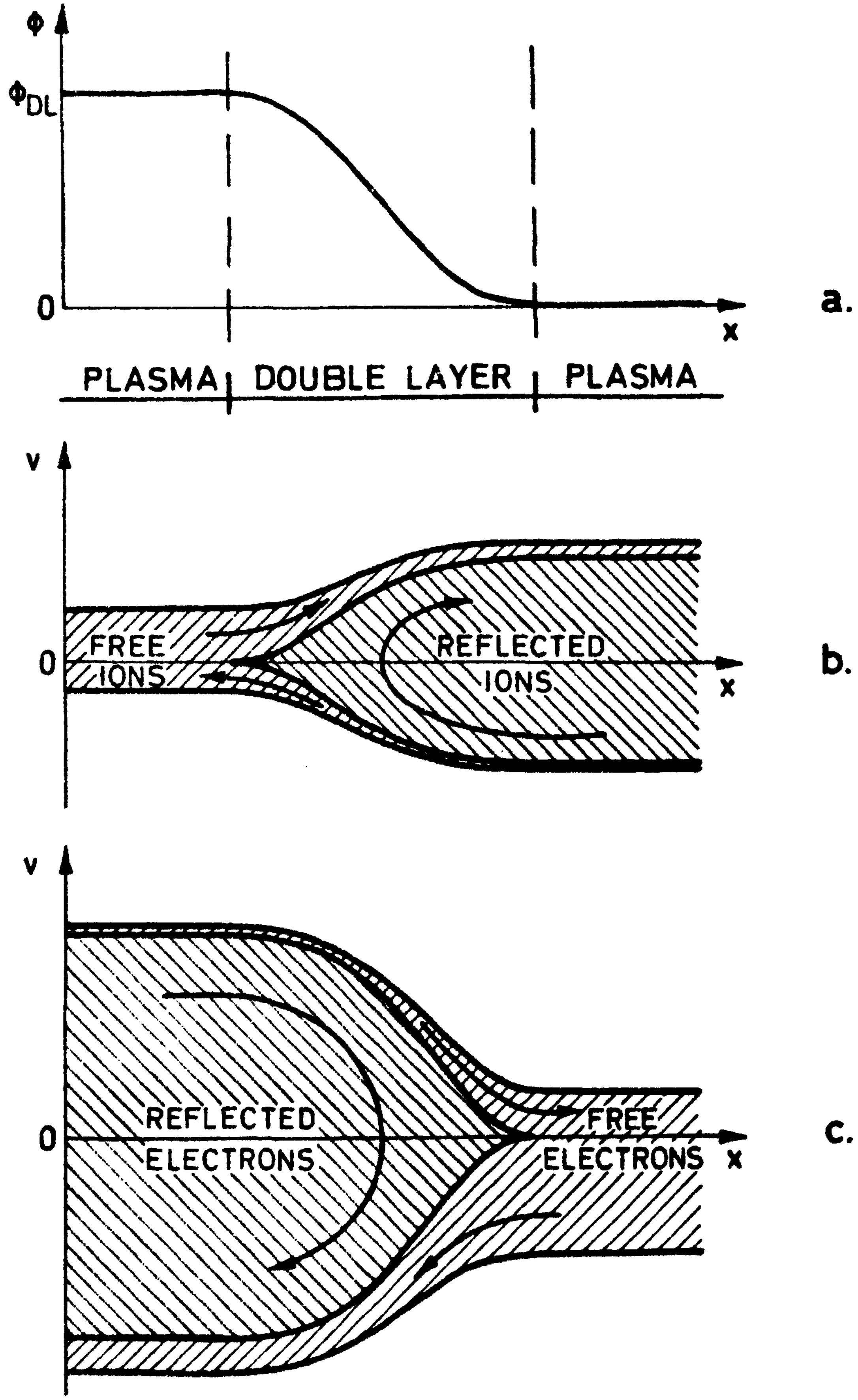
Φ
Φ_DL
0
x
a.
PLASMA
DOUBLE LAYER
PLASMA
v
FREE
IONS
REFLECTED
IONS
0
x
b.
v
REFLECTED
ELECTRONS
FREE
ELECTRONS
0
x
c.

Fig. 1

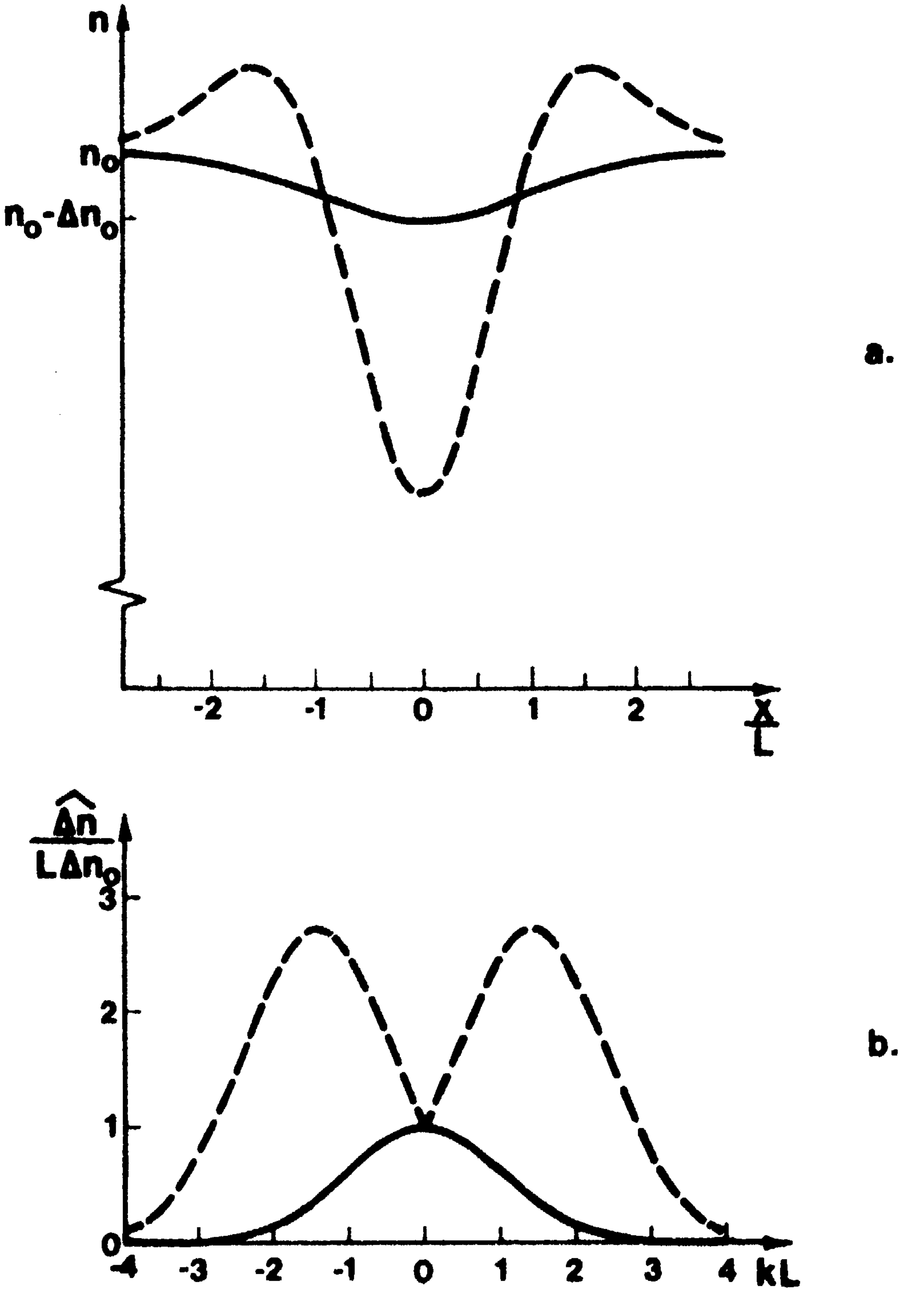
n
n_o
$n_o - \Delta n_o$
-2
-1
0
1
2
$\frac{x}{L}$
a.
$\frac{\widehat{\Delta n}}{L \Delta n_o}$
3
2
1
0
-4
-3
-2
-1
0
1
2
3
4
kL
b.

Fig. 2

t=0.00 L/c_i

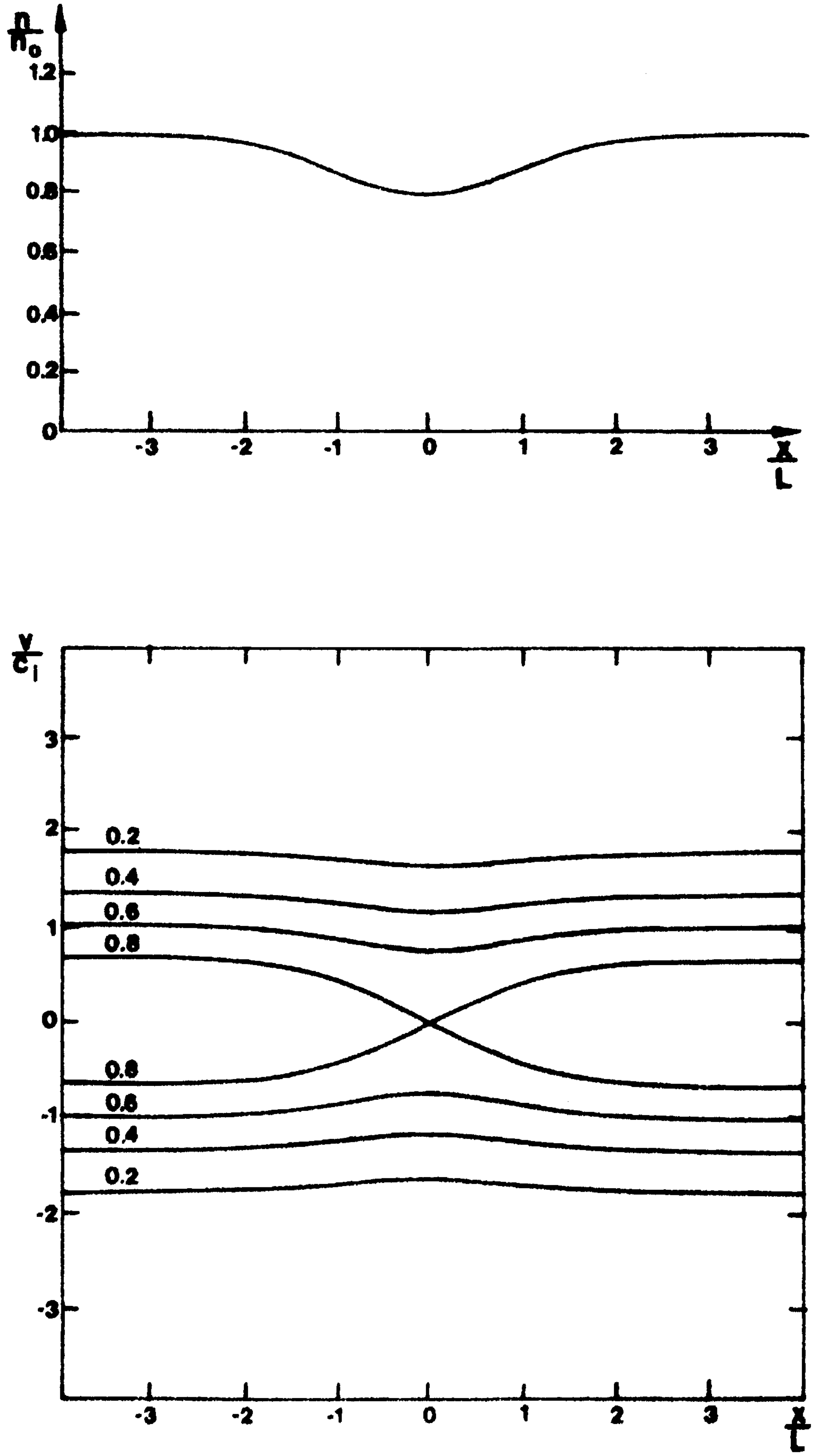

Fig. 3

$t = 0.53\ L/c_i$

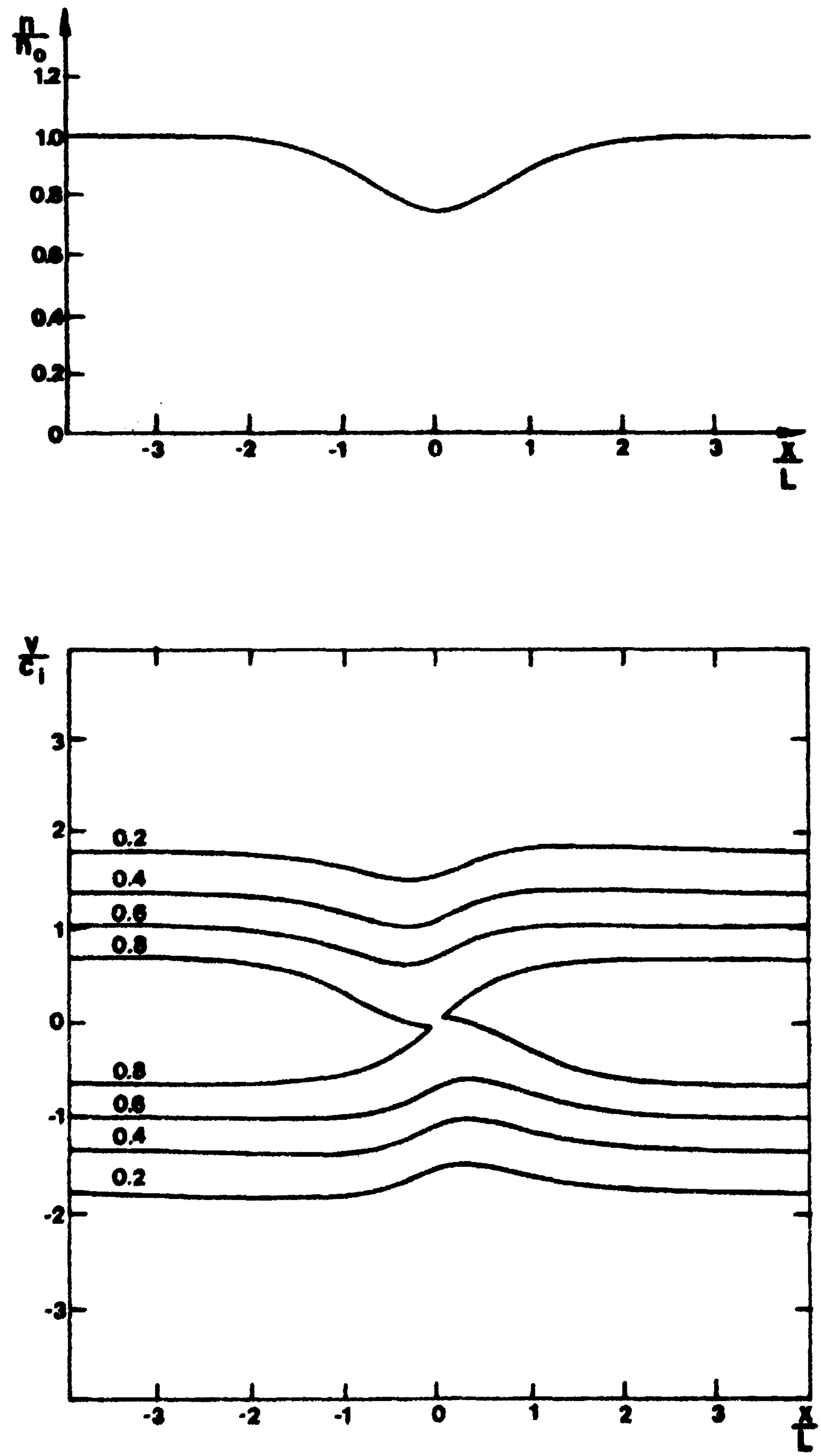

Fig.4

$t = 0.70\ L/c_i$

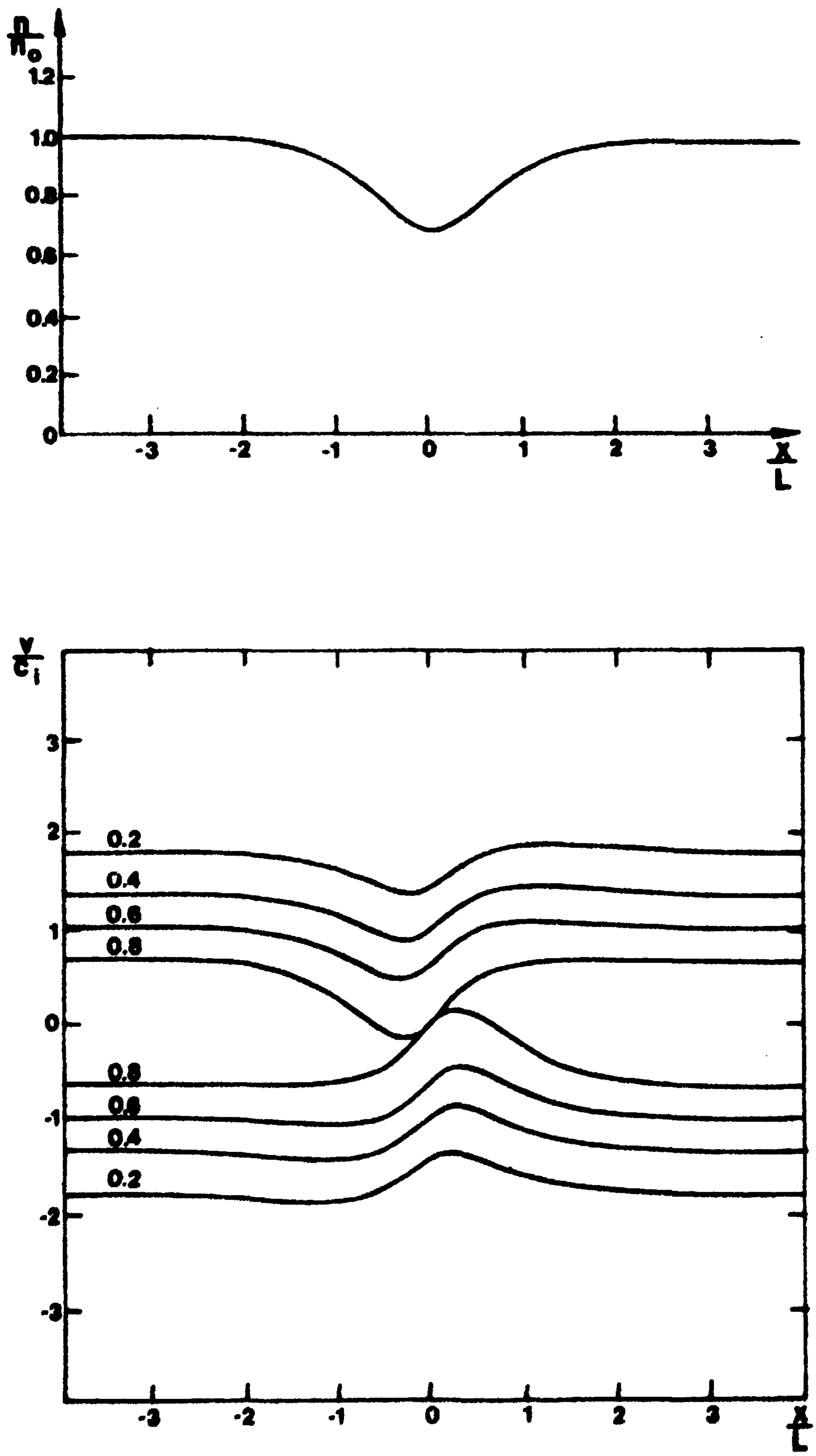

Fig. 5

$t = 0.88\ L/c_i$

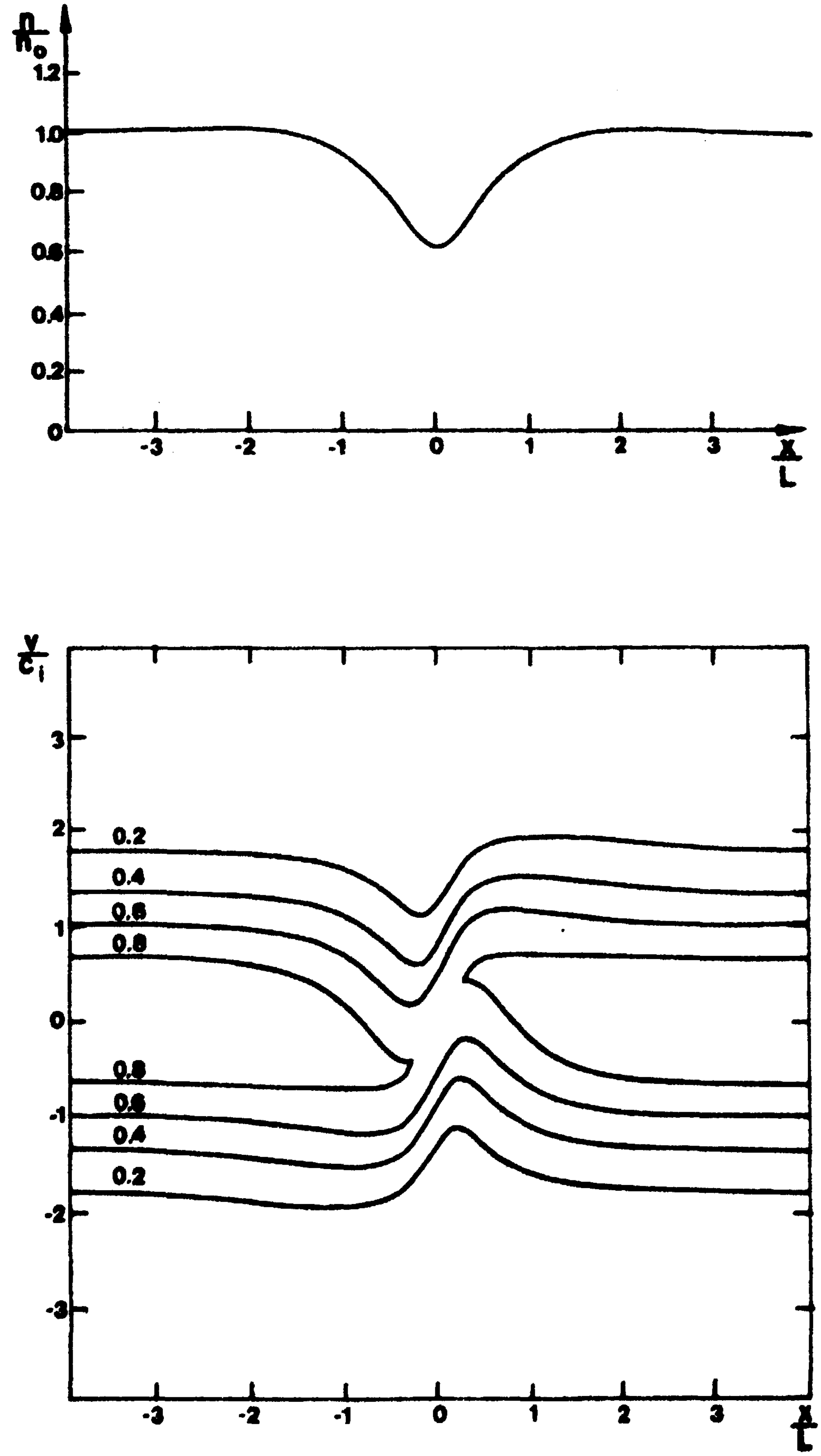

Fig. 6

t = 1.03 L/c_i

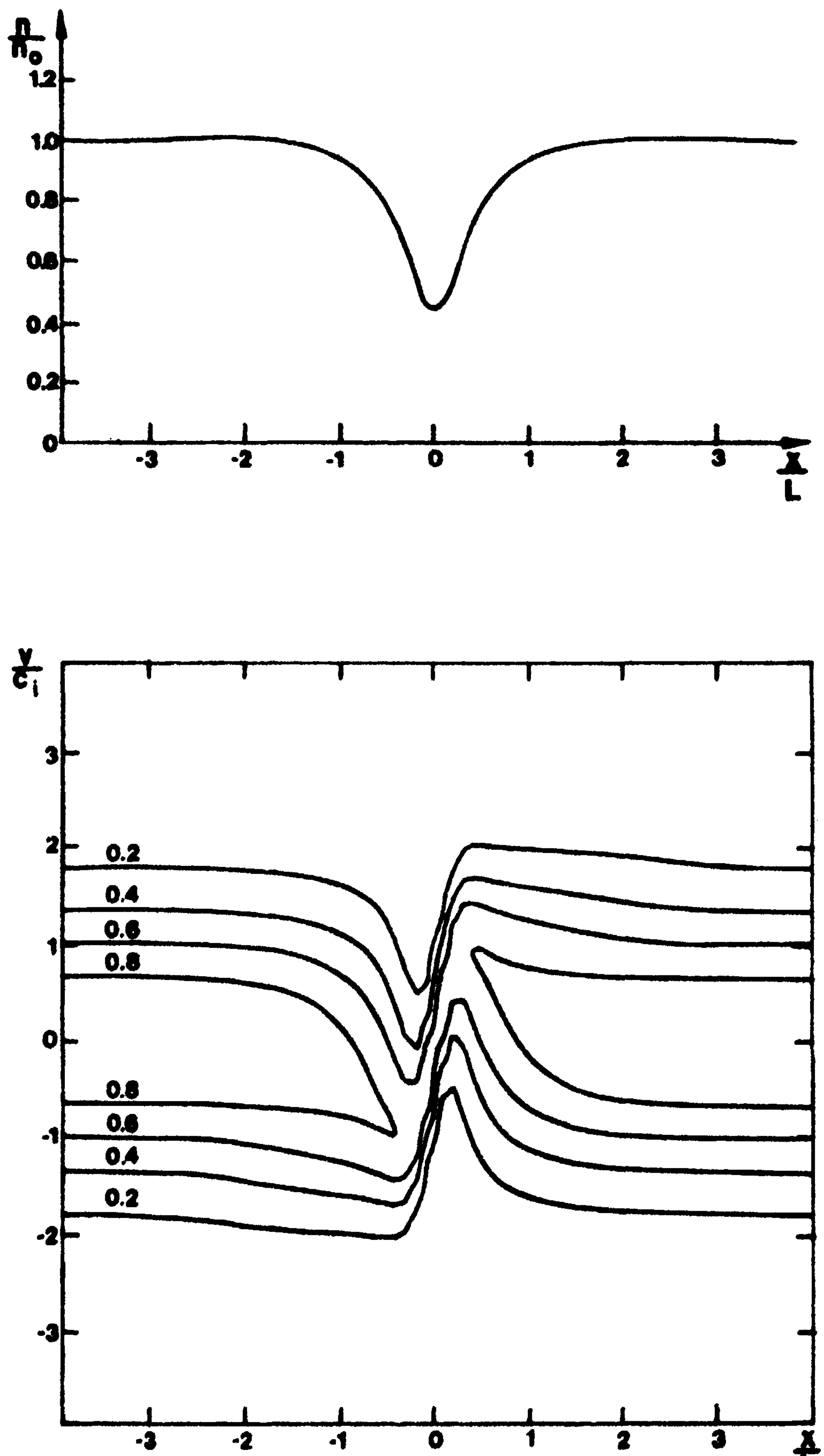

Fig. 7

t = 1.08 L/c_i

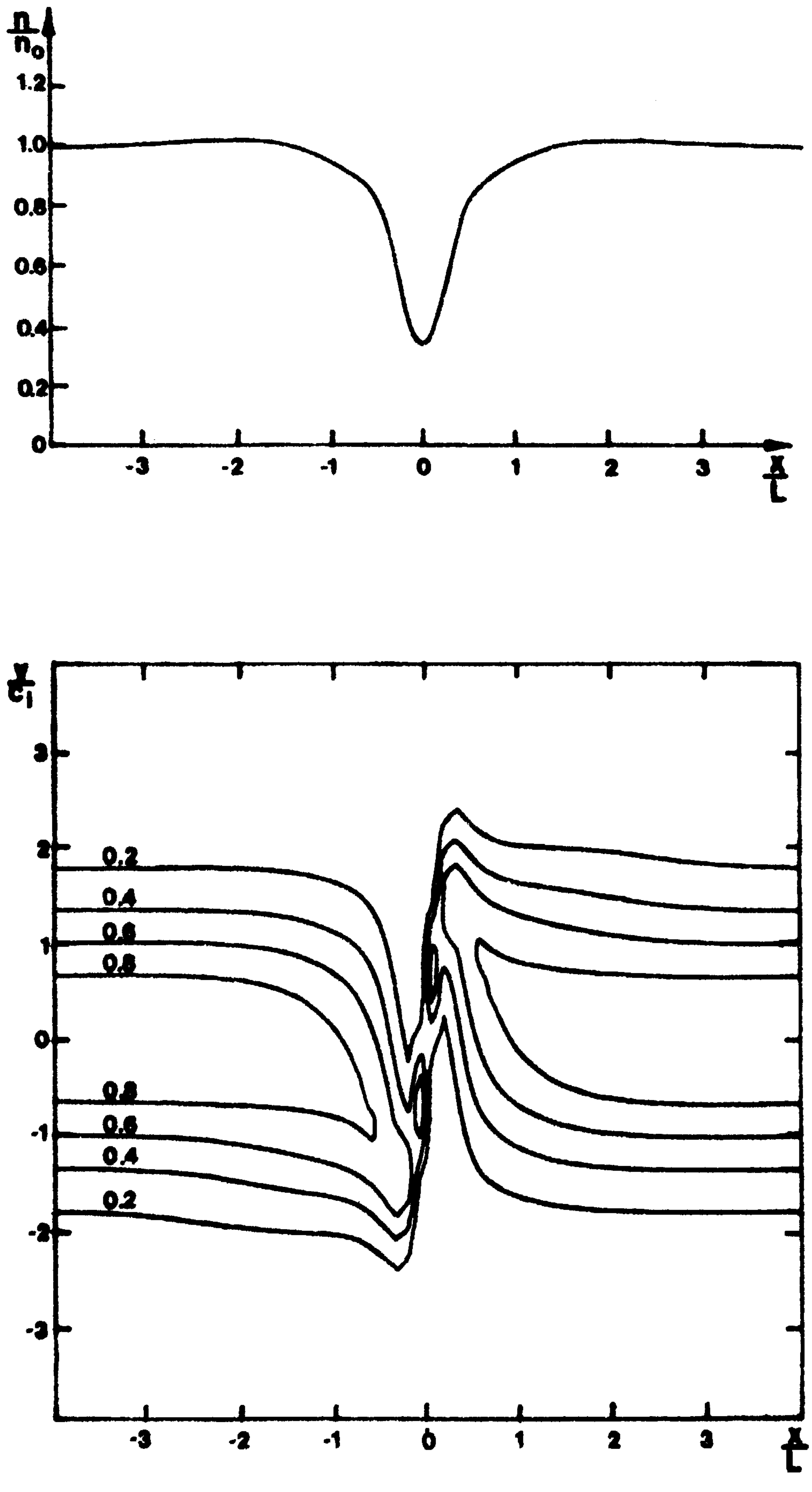

Fig. 8

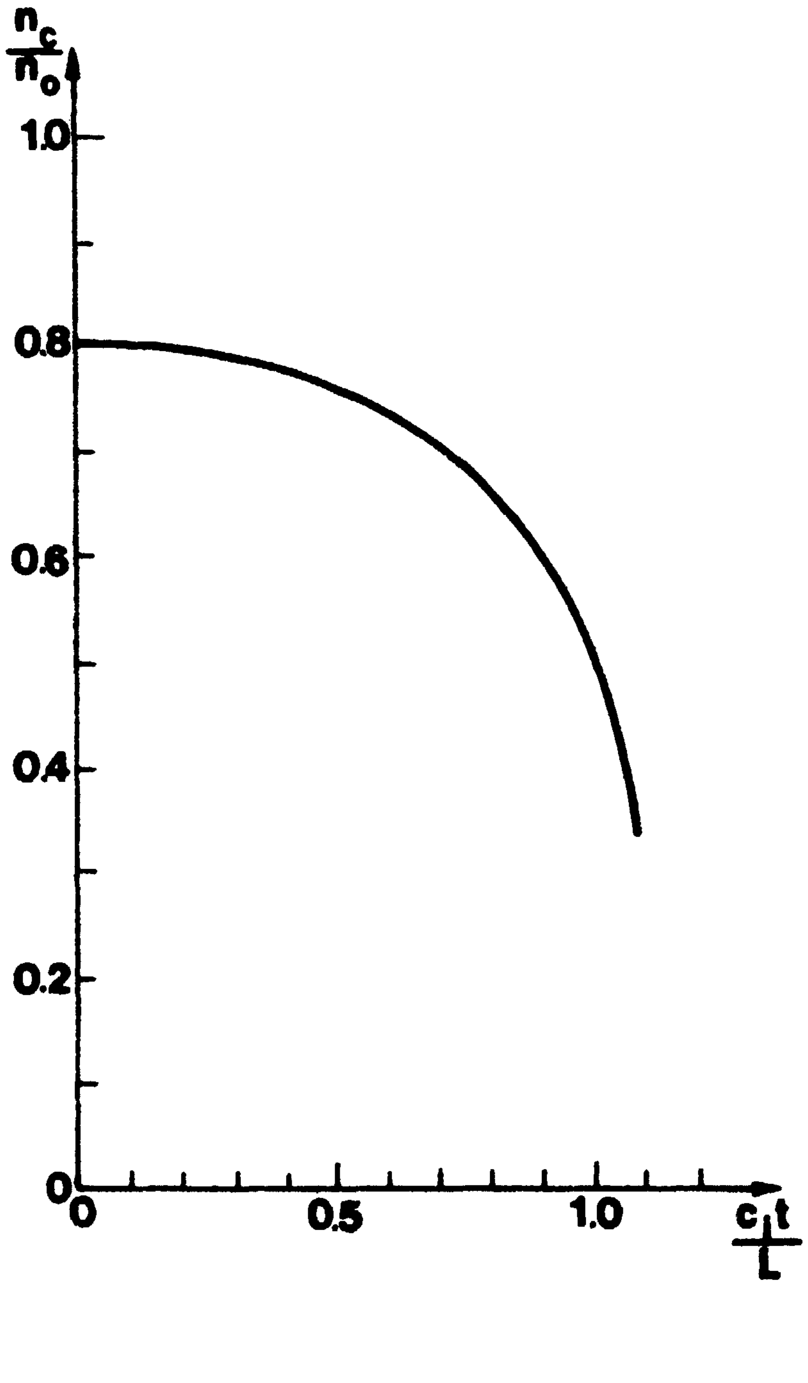

Fig. 9

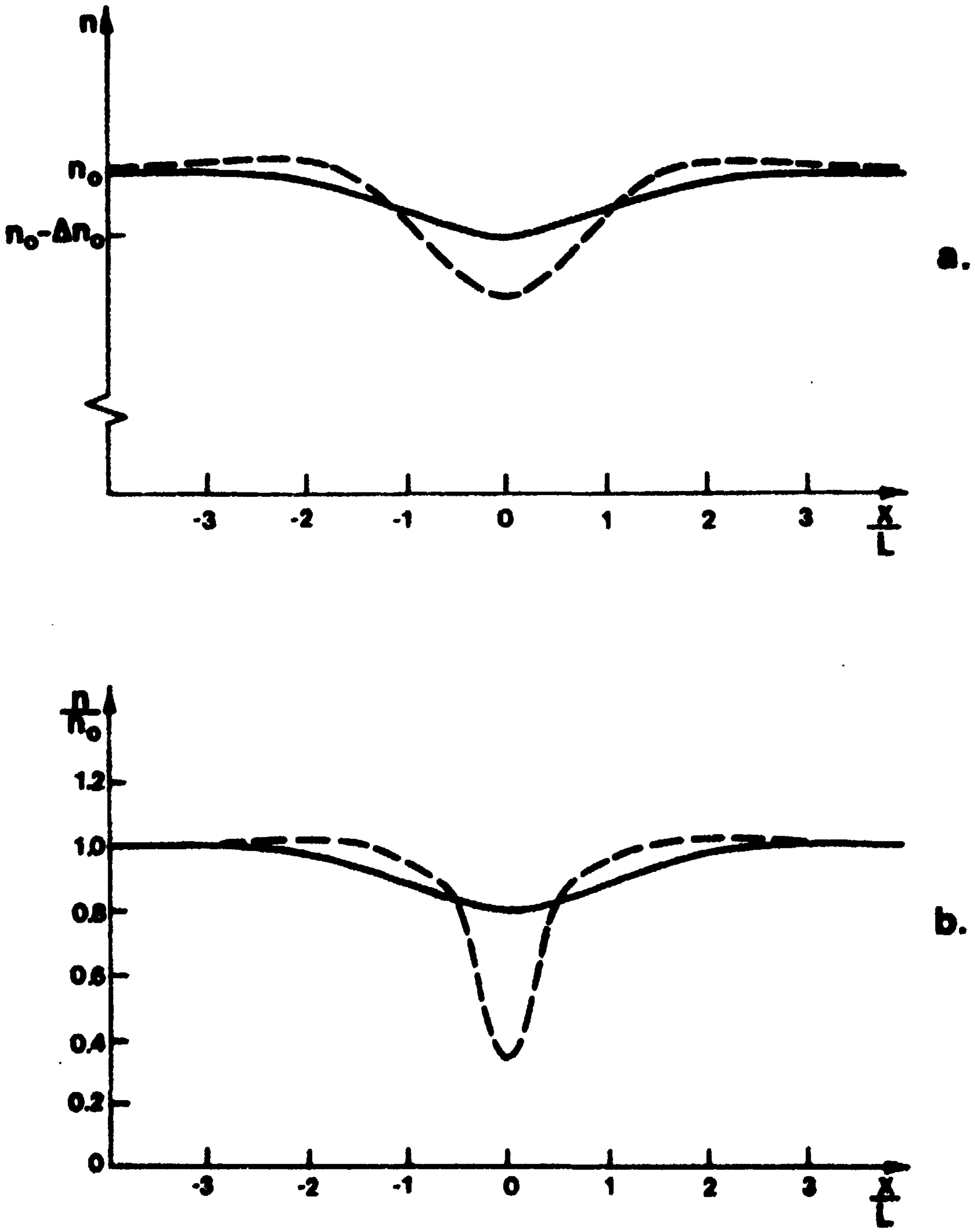

Fig. 10

TRITA-EPP-79-21

Royal Institute of Technology, Department of Plasma Physics,
Stockholm, Sweden

ELECTROSTATIC DOUBLE LAYERS AND A PLASMA EVACUATION PROCESS

M.A. Raadu and P. Carlqvist

December 1979, 34 pp. incl. illus., in English

An evacuation process due to the growth of current driven instabilities in a plasma is discussed. The process, which leads to localized extreme density reductions, is related to the formation of electrostatic double layers. The initial linear phase is treated using the superposition of unstable plasma waves. In the long wave length, non-dispersive limit a density dip, which is initially present as a small disturbance, grows rapidly and remains localized in the plasma. The process works for a variety of plasma conditions provided a certain current density is exceeded. For a particular choice of plasma parameters the non-linear development is followed, by solving the coupled Vlasov-Poisson equations by finite difference methods. The evacuation process is found to work even more effectively in the non-linear phase and leads to an extreme density reduction within the dip. It is suggested that the growth of such structures produces weak points within the plasma that can lead to the formation of double layers.

Key words: Double layers, Plasma evacuation, Plasma instabilities, Vlasov-Poisson equations, Finite difference methods, Cavitons, Anomalous resistivity.